Supporting Information Material

Intramolecular hydrogen bond-induced high chemical stability of metal-organic frameworks

Keke Wang, Qunmin Wang, Xiong Wang, Mei Wang, Qin Wang, Hai-Min Shen, Yun-Fang Yang and Yuanbin She*

State Key Laboratory Breeding Base of Green Chemistry-Synthesis Technology, College of Chemical Engineering, Zhejiang University of Technology, Hangzhou 310014, China

E-mail: sheyb@zjut.edu.cn

Table of Contents

Section S1. Materials and Instruments

All general reagents and solvents are commercially available and used without further purification.

Powder X-ray diffraction (PXRD) patterns were recorded with a Bruker D8 focusdiffractometer in a reflection mode. The two-theta angle ranges from 5º to 50º scanned with a step size of 0.02º. Nitrogen sorption experiment at 77 K was carried out using Micromeritics Analyzer (ASAP2460). The surface areas were determined by N_2 adsorption measurements according to BET model. Thermal gravimetric analysis (TGA) was carried out in air atmosphere using NETZSCH STA 449 instrument with a heating rate of 10 °C/min. X-ray photoelectron spectroscopy (XPS) was used to determine the binding energies of N by ESCALAB 250 (Thermo Fisher Scientific). The morphologies of the MOFs were characterized using a Hitachi S-4700 scanning electron microscope (SEM). The FT-IR spectroscopy was recorded on Nicolet 6700 FTIR spectrophotometer. The slice was made with powder constituted of KBr and sample by a tablet machine and the spectra data were recorded from 4000 to 400 cm^{-1}. Elemental analysis was carried out by using Vario EL cube Elemental Analyzer.

Section S2. Experiment procedures

2.1 Synthesis of Ligands

The synthetic paths to 3,3'-diamino-1,1'-biphenyl-4,4'-dicarboxylic acid (H_2BPDC-*o*-(NH_2)$_2$) and 2,2'-diamino-1,1'-biphenyl-4,4'-dicarboxylic acid (H_2BPDC-*m*-(NH_2)$_2$) are shown in Fig. S1.[1-3]

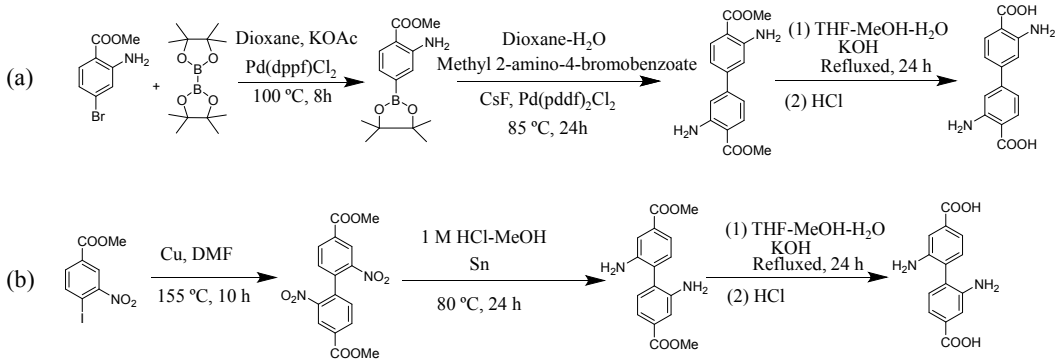

Fig. S1 Synthetic paths to (a) H_2BPDC-*o*-(NH_2)$_2$ and (b) H_2BPDC-*m*-(NH_2)$_2$.

2.1.1 Synthesis of H_2BPDC-*o*-(NH_2)$_2$

3-Amino-4-methoxycarbonyl-phenylboronic acid pinacol ester

Methyl 2-amino-4-bromobenzoate (32.4 g, 150.0 mmol), bis(pinacolato)diboron (32.4 g, 150.0 mmol), CH_3COOK (44.1 g, 450.0 mmol), [1,1'-bis(diphenylphosphino)ferrocene]dichloridepalladium(II) ($Pd(dppf)_2Cl_2$, 0.86 g, 1.0 mmol) and 1,4-dioxane (600 mL) were added to a round-bottom flask (1000 mL). Then the mixture was stirred at 100 ºC for 8 h under an atmosphere of nitrogen. After the cool-down, the product was mixed with deionized water (500 mL), and extracted with CH_2Cl_2. The organic layer was dried over Na_2SO_4 and evaporated to give crude residue. The column chromatography of the residue with mixture of hexanes and ethyl acetate (v/v = 10:1) as eluent gave 3-amino-4-methoxycarbonyl-phenylboronic acid pinacol

ester (28.6 g, yield: 68.6 %).[1]H NMR (600 MHz, $CDCl_3$; δ, ppm): 7.85 (d, 1H), 7.13 (s, 1H), 7.05 (dd, 1H), 3.87 (s, 3H), 1.34 (s, 12H).[4]

Dimethyl 3,3'-diamino-1,1'-biphenyl-4,4'-dicarboxylate

3-Amino-4-methoxycarbonyl-phenylboronic acid pinacol ester (20.0 g, 76.0 mmol), methyl 2-amino-4-bromobenzoate (19.6 g, 91.2 mmol), CsF (35.0 g, 228.0 mmol), $Pd(dppf)_2Cl_2$ (0.30 g, 0.42 mmol), and 1,4-dioxane/H_2O (400 mL, v/v = 1:1) were added to a round-bottom flask (1000 mL). Then the mixture was stirred at 85 ºC for 24 h under an atmosphere of nitrogen. After the cool-down, the product was extracted with CH_2Cl_2. The organic layer was dried over Na_2SO_4 and evaporated to give crude residue. The column chromatography of the residue with mixture of CH_2Cl_2 and hexanes (v/v = 10:1) as eluent gave dimethyl 3,3'-diamino-1,1'-biphenyl-4,4'-dicarboxylate (14.6 g, yield: 64.6%). [1]H NMR (600 MHz, DMSO-d_6; δ, ppm): 7.78 (d, 2H), 7.03 (d, 2H), 6.77 (dd, 2H), 3.80 (s, 6H).[1]

H_2BPDC-o-$(NH_2)_2$

Dimethyl 3,3'-diamino-1,1'-biphenyl-4,4'-dicarboxylate (6.3 g, 21.0 mmol) was dissolved in THF/MeOH (40 mL, v/v =1:1). An aqueous solution (60 mL) of KOH (4.6 g, 81 mmol) was added to the mixture. Then the mixture was refluxed for 24 h. After the cool-down, the organic solvent was removed. Deionized water (100 mL) was added. Then the filtrate was collected and acidified until pH reachs 5.0. The formed precipitate was collected, washed with water, and dried to obtain H_2BPDC-*o*-$(NH_2)_2$ (5.3 g, yield: 94.4%). [1]H NMR (600 MHz, DMSO-d_6; δ, ppm): 7.77 (d, 2H), 6.99 (d, 2H), 6.75 (dd, 2H).[1]

2.1.2 Synthesis of H_2BPDC-*m*-$(NH_2)_2$

Cu powder activation

Cu powder (100 g) was treated with a 2% solution of iodine (I_2) dissolved in acetone (1000 mL) at room temperature for 10 min. After filtration, the Cu powder was washed thoroughly with acetone/concentrated hydrochloric acid solution (v/v = 1:1, 500 mL). The Cu powder was filtered and washed with acetone until pH of the filtrate reachs 7. Then, the Cu powder was dried under reduced pressure at 60 ºC for 24 h.

Dimethyl 2,2'-dinitro-[1,1'-biphenyl]-4,4'-dicarboxylate

Methyl 4-iodo-3-nitrobenzoate (24.56 g, 80.0 mmol), activated Cu powder (51.20 g, 800 mmol), and DMF (40.0 mL) were added to a round-bottom flask (100 mL). The mixture was kept at 155 ºC for 10 hours under an atmosphere of nitrogen. Then the hot mixture was directly filtered. The obtained filtrate was added into stirred deionized water (1000 mL). Then the precipitate was collected and purified with column chromatography (silica gel, CH_2Cl_2/hexanes (v/v = 1:1)) to obtain dimethyl 2,2'-dinitro-[1,1'-biphenyl]-4,4'-dicarboxylate (10.45 g, yield: 72.5%). ^{1}H NMR (600 MHz, $CDCl_3$; δ, ppm): 8.92 (s, 2H), 8.38 (d, 2H), 7.41 (d, 2H), 4.04 (s, 6H).[5]

Dimethyl 2,2'-diamino-1,1'-biphenyl-4,4'-dicarboxylate

Dimethyl 2,2'-dinitro-[1,1'-biphenyl]-4,4'-dicarboxylate (10.00 g, 27.80 mmol), tin powder (21.60 g, 334.0 mmol), 1 M HCl (300 mL), and methanol (500 mL) were added into a round-bottom flask. The mixture was kept at 80 ºC overnight under an atmosphere of nitrogen. The mixture was cooled to room temperature and poured onto

cold 2 M NaOH (400 mL) to obtain yellow solid. The precipitate was collected and dissolved in ethyl acetate (1000 mL) followed by filtration to remove undissolved solid. The filtrate was evaporated under vacuum to yield the product as a yellow solid, which was recrystallized by isopropanol (3.3 g, yield: 39.5%). ^{1}H NMR (600 MHz, $CDCl_3$; δ, ppm): 7.50 (dd, 2H), 7.48 (s, 2H), 7.19 (d, 2H), 3.92 (s, 6H).[3]

H_2BPDC-m-$(NH_2)_2$

H_2BPDC-*m*-$(NH_2)_2$ was synthesized by hydrolysis of dimethyl 3,3'-diamino-1,1'-biphenyl-4,4'-dicarboxylate and subsequent acidification. The detail procedure is similar to the synthesis of H_2BPDC-*o*-$(NH_2)_2$. The yield is 93.1%. ^{1}H NMR (600 MHz, DMSO-d_6; δ, ppm): 7.42 (s, 2H), 7.22 (d, 2H), 7.06 (d, 2H).[2]

2.2 Synthesis of MOFs

2.2.1 Synthesis of UiO-67-*o*-$(NH_2)_2$

$ZrCl_4$ (0.233 g, 1.0 mmol) and acetic acid (7.206 g, 120 mmol) were dissolved in DMF (40 mL) followed by 10 min of ultrasound. H_2BPDC-*o*-$(NH_2)_2$ (0.272 g, 1.0 mmol) was added to the solution. After 10 min of ultrasound, the mixture was sealed, heated to 120 ºC, and held at the temperature for 24 h. After being cooled to room temperature, the as-synthesized UiO-67-*o*-$(NH_2)_2$ solid was obtained by centrifugation. Clear mother liquid was decanted.

To activate the UiO-67-*o*-$(NH_2)_2$, the solid was washed by DMF (3 × 60 mL) over an eight-hour period. Then the DMF was replaced with methanol (6 × 60 mL) over a four-hour period. Finally, the solid was dried at 120 ºC under vacuum overnight to

obtain activated UiO-67-*o*-$(NH_2)_2$. EA calculated: C, 43.70%; H: 2.78%; N: 7.28%. Found: C, 43.54%; H, 2.83%; N, 7.25%.

2.2.2 Synthesis of UiO-67-*m*-$(NH_2)_2$

The synthesis and activation of UiO-67-*m*-$(NH_2)_2$ are similar to those of UiO-67-*o*-$(NH_2)_2$ by replacing H_2BPDC-*o*-$(NH_2)_2$ with H_2BPDC-*m*-$(NH_2)_2$. EA calculated: C, 43.70%; H: 2.78%; N: 7.28%. Found: C, 43.38%; H, 2.85%; N, 7.24%.

2.2.3 Synthesis of UiO-67

$ZrCl_4$ (0.117 g, 0.5 mmol), 4,4'-biphenyldicarboxylic acid (H_2BPDC) (0.121 g, 0.5 mmol), benzoic acid (1.832 g, 15.0 mmol), and DMF (20 mL) were added to a Teflon liner (100 mL). After 10 min of sonication, the reaction mixture was kept at 120 ºC for 24 h, then cooled to room temperature. The resulting UiO-67 was collected by centrifugation, washed with DMF and acetone five times, and dried under vacuum at 120 ºC for 12 h. EA calculated: C, 47.41%; H: 2.45%. Found: C, 47.50%; H, 2.65%.

2.3 Stability test

MOFs (0.080 g) were immersed in water, pH = 2 HCl solution, and pH = 12 NaOH solution (8 mL) for 24 h. Then the solids were collected by centrifugation, washed with H_2O three times. Finally, these treated solids were dried at 120 ºC for 12 h.

Section S3. Calculation method

3.1 Calculation on ligands

All the calculations were carried out with the Gaussian 09 package.[6] Geometry optimization and energy calculations were performed with the B3LYP method. The 6-31G(d) basis set was used for all atoms. The configurations with different carboxyl group-aromatic ring torsion angle in ligands were obtained.

The pK_a calculations were computed at the B3LYP-D3/Def2TZVP level of the theory on gas phase optimized geometries in dimethylsulfoxide with the application of the SMD solvation model.[7,8]

3.2 Calculation on MOFs

Density functional theory (DFT) calculations were performed to calculate the partial charges of the framework atoms of UiO-67-*o*-$(NH_2)_2$ and UiO-67-*m*-$(NH_2)_2$ by cleaving representative clusters from their respective unit cells, which were saturated with hydrogen to minimize the boundary effects. The electrostatic potential (ESP) charges obtained by ChelpG method were used as the atomic partial charges. The DFT calculations were carried out using the Gaussian 09 suite of quantum mechanical program with the Perdew-Burke-Ernzerhof (PBE) exchange and correlation functional. Geometry optimizations and the single-point energy calculations were performed at the Becke three parameters hybrid exchange-correlation functional (B3LYP) level of theory.[9] The basis set LANL2DZ was employed for Zr atoms, and 6-31+G* was used for the rest of the atoms (C, H, O, N). To account for weak interactions, the dispersion

correction schemes for Grimme (denoted as D3) were used.[10]

For the geometry optimization procedure, the structures were optimized until the forces were < 10^{-5} hartree/bohr and the energy change was 10^{-7} hartree. The convergence criterion for the energy calculation during the self-consistent-field procedure was set for 10^{-8} hartree. The above methods have been employed widely to estimate the atomic partial charges and energies in numbers of MOFs.[11,12] The configurations with different degree of rotation the ligands in the Zr_6 cluster were obtained by changing the angle between the carboxylate group and the adjacent aromatic ring in the cluster model.

Section S5. Characterization results

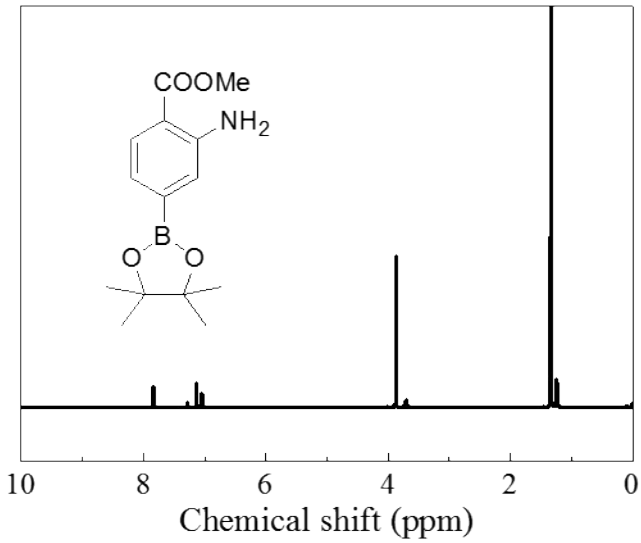

Fig. S2 ^{1}H NMR ($CDCl_3$, 600 MHz) spectrum of 3-amino-4-methoxycarbonyl-phenylboronic acid pinacol ester.

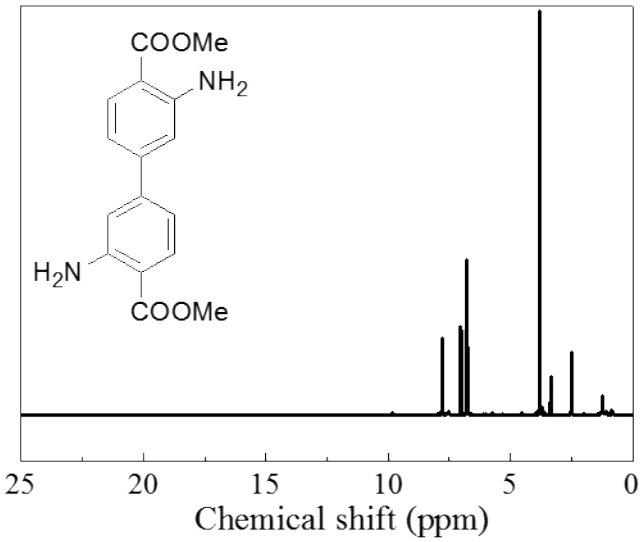

Fig. S3 ^{1}H NMR (DMSO-d_6, 600 MHz) spectrum of dimethyl 3,3'-diamino-1,1'-biphenyl-4,4'-dicarboxylate.

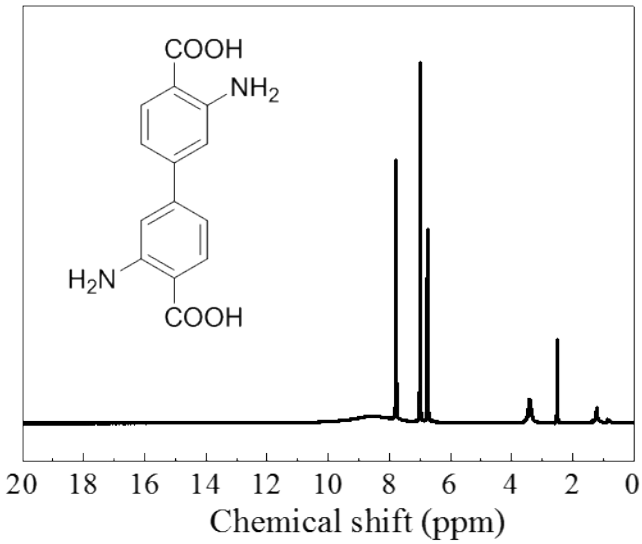

Fig. S4 ^{1}H NMR (DMSO-d_6, 600 MHz) spectrum of H_2BPDC-*o*-$(NH_2)_2$.

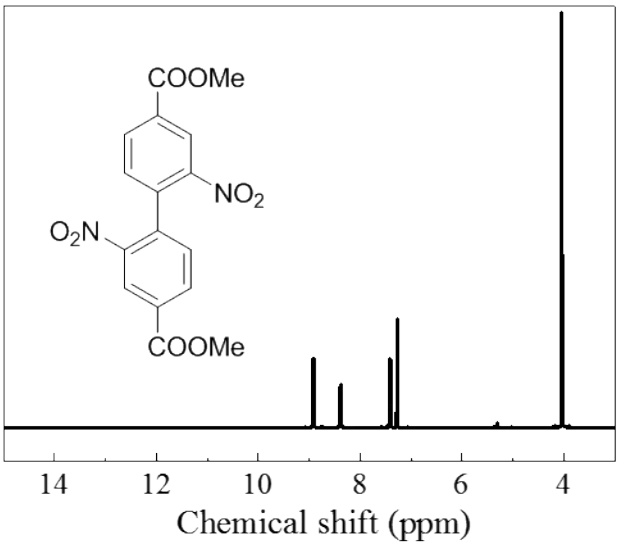

Fig. S5 ^{1}H NMR ($CDCl_3$, 600 MHz) spectrum of dimethyl 2,2'-dinitro-[1,1'-biphenyl]-4,4'-dicarboxylate.

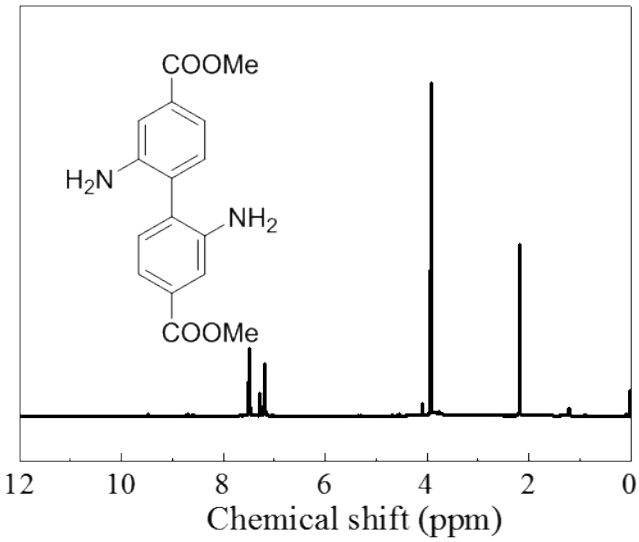

Fig. S6 ^{1}H NMR ($CDCl_3$, 600 MHz) spectrum of dimethyl 2,2'-diamino-1,1'-biphenyl-4,4'-dicarboxylate.

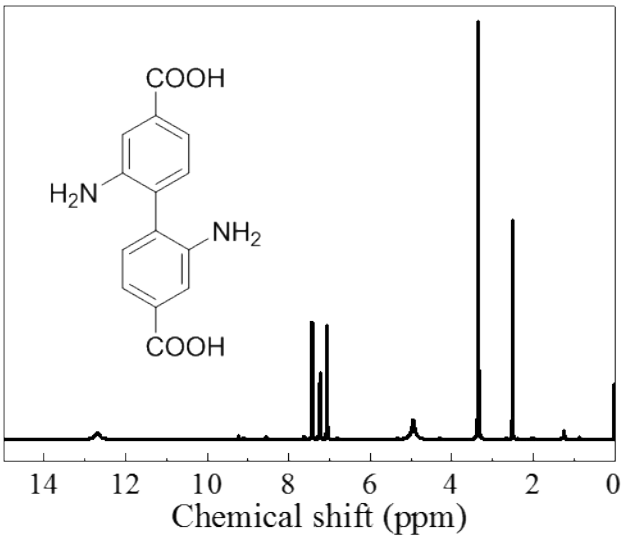

Fig. S7 ^{1}H NMR (DMSO-d_6, 600 MHz) spectrum of H_2BPDC-*m*-$(NH_2)_2$.

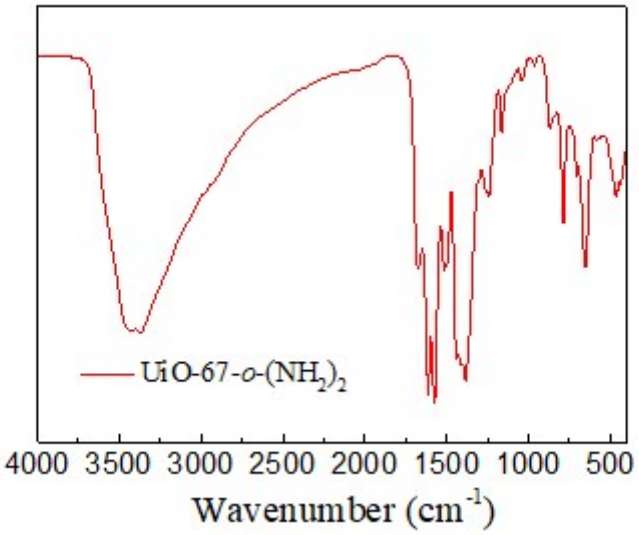

Fig. S8 FT-IR spectrum of UiO-67-*o*-$(NH_2)_2$.

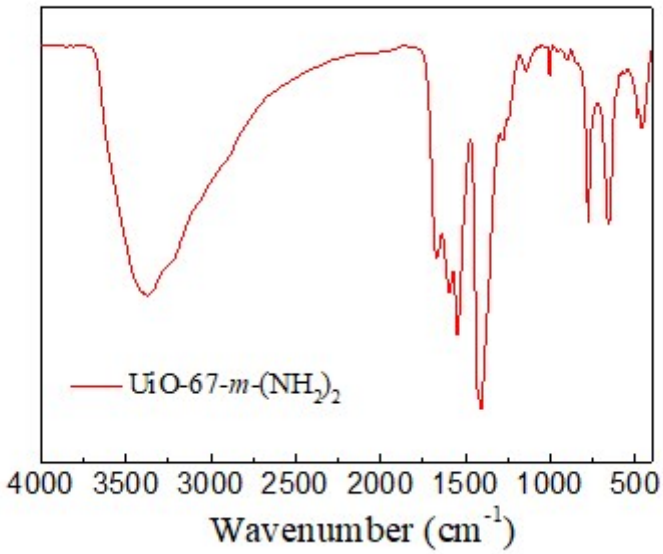

Fig. S9 FT-IR spectrum of UiO-67-*m*-$(NH_2)_2$.

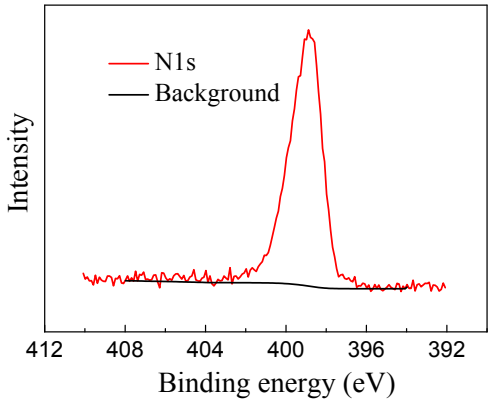

Fig. S10 XPS spectrum of N1s of UiO-67-*o*-$(NH_2)_2$.

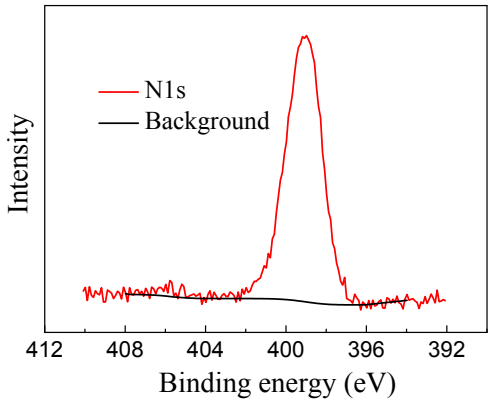

Fig. S11 XPS spectrum of N1s of UiO-67-*m*-$(NH_2)_2$.

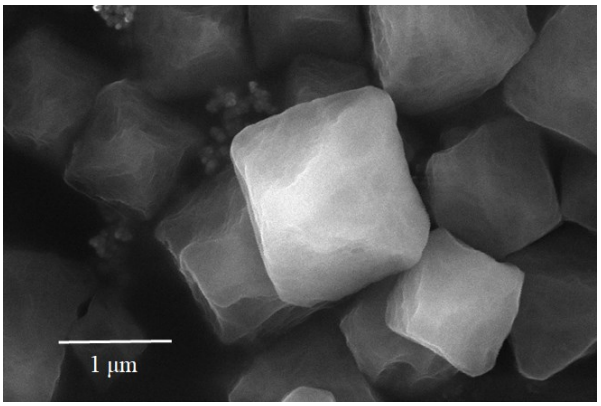

Fig. S12 SEM picture of UiO-67-*o*-$(NH_2)_2$.

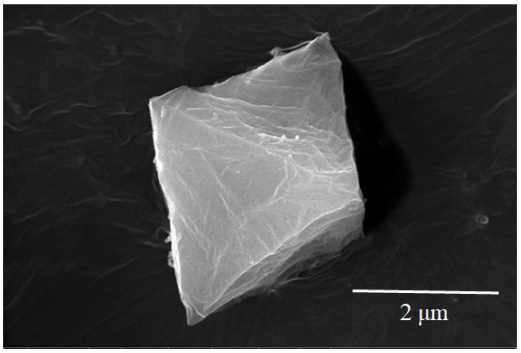

Fig. S13 SEM picture of UiO-67-*m*-$(NH_2)_2$.

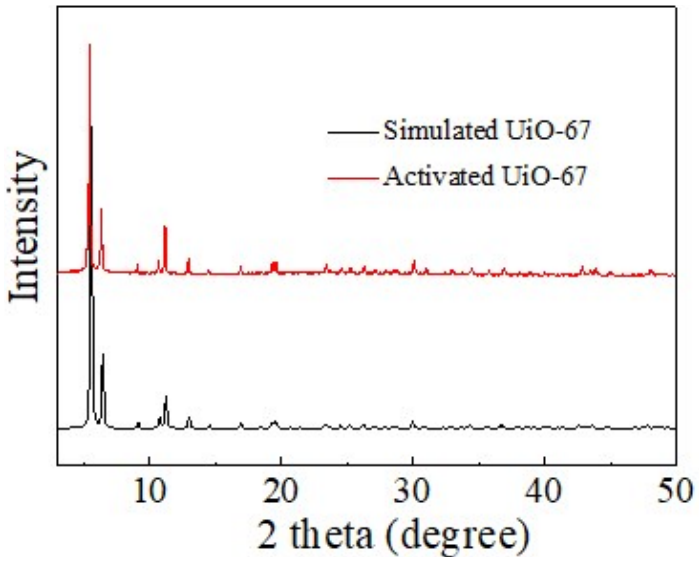

Fig. S14 PXRD pattern of UiO-67.

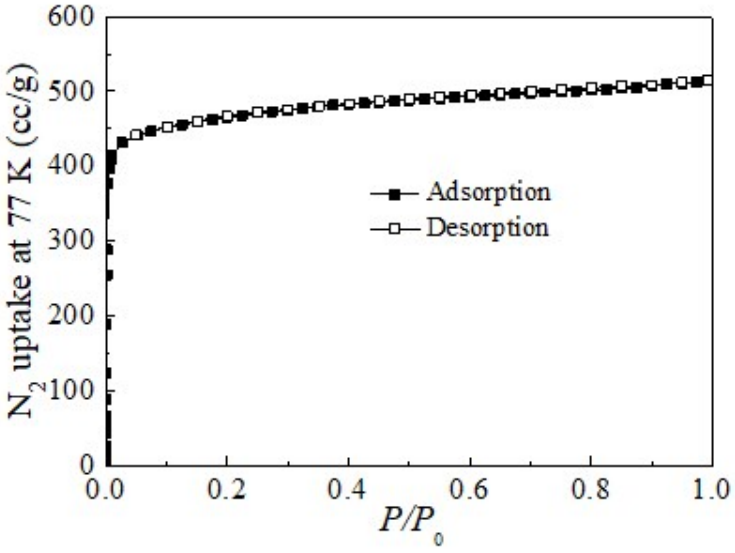

Fig. S15 N_2 sorption isotherms of UiO-67 at 77 K.

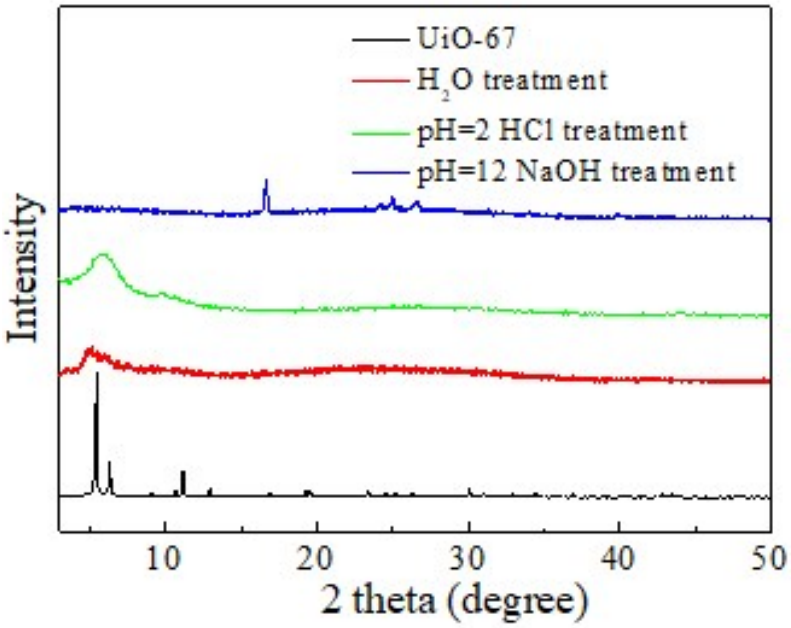

Fig. S16 PXRD patterns of UiO-67 treated in H_2O, pH = 2 HCl solution, and pH = 12 NaOH solution.

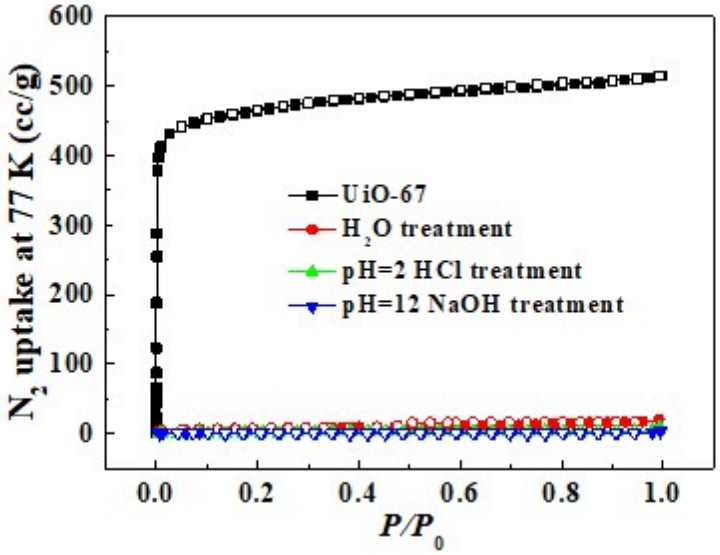

Fig. S17 N_2 sorption isotherms at 77 K of UiO-67 before and after treatment with H_2O, pH = 2 HCl solution, and pH = 12 NaOH solution.

Section S5. Calculation results

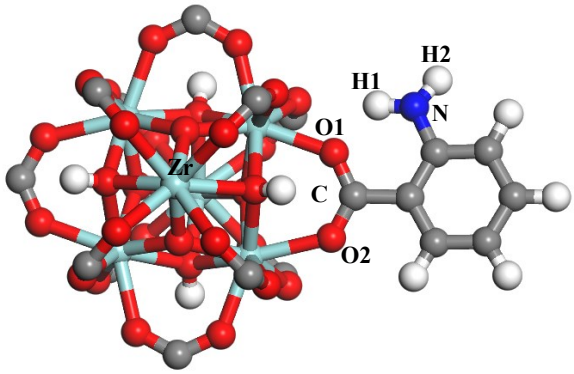

Fig. S18 Cluster used for calculating the partial charges for atoms of the UiO-67-*o*-$(NH_2)_2$. The terminations of the cluster were saturated with hydrogen to minimize the boundary effects.

Table S1 Atomic partial charges for the UiO-67-*o*-$(NH_2)_2$ structure.

Atomic type	Zr1	O1	O2	C1	N1	H1	H2
Charge (e)	2.471	-0.741	-0.721	0.846	-0.867	0.389	0.361

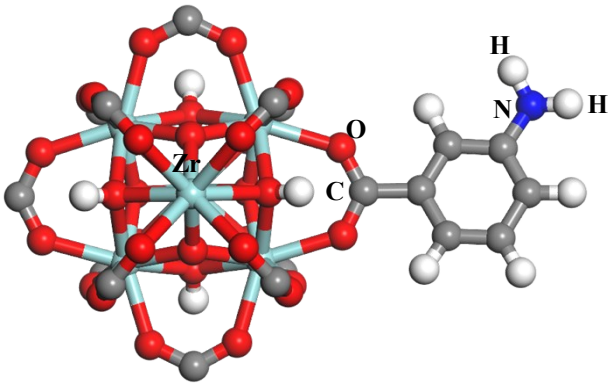

Fig. S19 Cluster used for calculating the partial charges for atoms of the UiO-67-*m*-$(NH_2)_2$. The terminations of the cluster were saturated with hydrogen to minimize the boundary effects.

Table S2 Atomic partial charges for the UiO-67-*m*-$(NH_2)_2$ structure.

Atomic type	Zr	O	C	N	H
Charge (e)	2.370	-0.725	0.819	-0.858	0.345

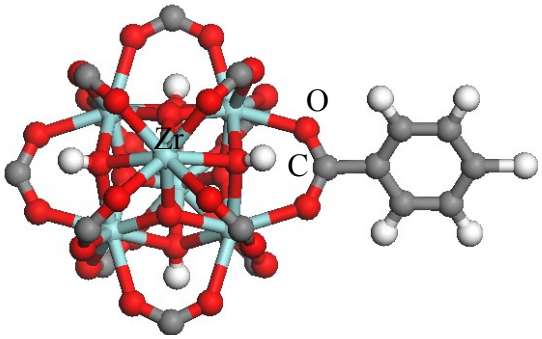

Fig. S20 Cluster used for calculating the partial charges for atoms of the UiO-67. The terminations of the cluster were saturated with hydrogen to minimize the boundary effects.

Table S3 Atomic partial charges for the UiO-67 structure.

Atomic type	Zr	O	C
Charge (e)	2.264	-0.691	0.786

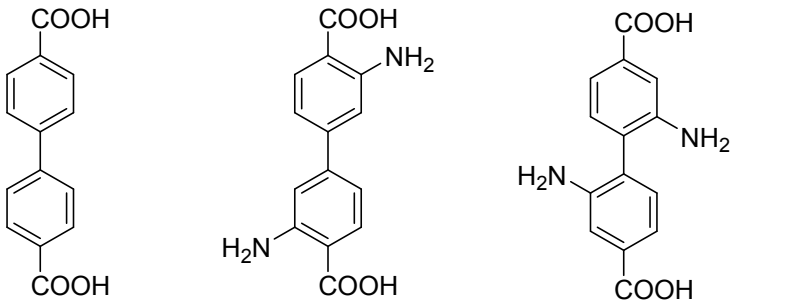

	H_2BPDC	H_2BPDC-*o*-$(NH_2)_2$	H_2BPDC-*m*-$(NH_2)_2$
pK_a	22.1	22.5	23.3

Fig. S21 The pKa values of H_2BPDC, H_2BPDC-*o*-$(NH_2)_2$, and H_2BPDC-*m*-$(NH_2)_2$.

Section S6. References

1. T.-Y. Luo, C. Liu, S. V. Eliseeva, P. F. Muldoon, S. Petoud and N. L. Rosi, Rare earth pcu metal-organic framework platform based on $Re_4(\mu_3\text{-}OH)_4(COO)_6^{2+}$ clusters: rational design, directed synthesis, and deliberate tuning of excitation wavelengths, *J. Am. Chem. Soc.*, 2017, **139**, 9333-9340.
2. N. Ko, J. Hong, S. Sung, K. E. Cordova, H. J. Park, J. K. Yang and J. Kim, A significant enhancement of water vapour uptake at low pressure by amine-functionalization of UiO-67, *Dalton Trans.*, 2015, **44**, 2047-2051.
3. P. V. Dau and S. M. Cohen, A bifunctional, site-isolated metal-organic framework-based tandem catalyst, *Inorg. Chem.*, 2015, **54**, 3134-3138.
4. Q. Shao, K. Liang, H. Ling, Y. Wang, Z. Yan, G. Xia and H. Wang, Tetraphenylethylene-incorporated squaraine dyes: structural and theoretical insights into the diverse emission behaviors in solution and solid state, *J. Mater. Chem. C*, 2020, **8**, 4549-4556.
5. P. V. Dau and S. M. Cohen, The influence of nitro groups on the topology and gas sorption property of extended Zn(II)-paddlewheel MOFs, *CrystEngComm*, 2013, **15**, 9304-9307.
6. M. J. Frisch, G. W. Trucks, H. B. Schlegel, G. E. Scuseria, M. A. Robb, J. R. Cheeseman, G. Scalmani, V. Barone, B. Mennucci, G. A. Petersson, H. Nakatsuji, M. Caricato, X. Li, H. P. Hratchian, A. F. Izmaylov, J. Bloino, G. Zheng, J. L. Sonnenberg, M. Hada, M. Ehara, K. Toyota, R. Fukuda, J. Hasegawa, M. Ishida, T. Nakajima, Y. Honda, O. Kitao, H. Nakai, T. Vreven, J. A. Montgomery, J. E. Peralta, F. Ogliaro, M. Bearpark, J. J. Heyd, E. Brothers, K. N. Kudin,V. N. Staroverov, R. Kobayashi, J. Normand, K. Raghavachari, A. Rendell, J. C. Burant, S. S. Iyengar, M. Tomasi, N. Cossi, J. M. Millam, M. Klene, J. E. Knox, J. B. Cross, V. Bakken, C. Adamo, J. Jaramillo, R. Gomperts, R. E. Stratmann, O. Yazyev, A. J. Austin, R. Cammi, C. Pomelli, J. W. Ochterski, R. L. Martin, K. Morokuma, V. G. Zakrzewski, G. A. Voth, P. Salvador, J. J. Dannenberg, S. Dapprich, A. D. Daniels, Ö. Farkas, J. B. Foresman, J. V. Ortiz, J. Cioslowski and D. J. Fox,

Gaussian 09 (Revision D.01), Gaussian Inc., Wallingford, CT, 2013.

7. B. Thapa and K. Raghavachari, Accurate p*K*a evaluations for complex bio-organic molecules in aqueous media, *J. Chem. Theory Comput.*, 2019, **15**, 6025-6035.
8. A. V. Marenich, C. J. Cramer and D. G. Truhlar, Universal solvation model based on solute electron density and on a continuum model of the solvent defined by the bulk dielectric constant and atomic surface tensions, *J. Phys. Chem. B*, 2009, **113**, 6378-6396.
9. P. J. Stephens, F. J. Devlin, C. F. Chabalowski and M. J. Frisch, Ab initio calculation of vibrational absorption and circular dichroism spectra using density functional force fields, *J. Phys. Chem.*, 1994, **98**, 11623-11627.
10. S. Grimme, J. Antony, S. Ehrlich and H. Krieg, A consistent and accurate ab initio parametrization of density functional dispersion correction (DFT-D) for the 94 elements H-Pu, *J. Chem. Phys.*, 2010, **132**, 154104.
11. S. T. Meek, S. L. Teich-McGoldrick, J. J. Perry IV, J. A. Greathouse and M. D. Allendorf, Effects of polarizability on the adsorption of noble gases at low pressures in monohalogenated isoreticular metal-organic frameworks, *J. Phys. Chem. C*, 2012, **116**, 19765-19772.
12. Q. Yang, A. D. Wiersum, P. L. Llewellyn, V. Guillerm, C. Serre and G. Maurin, Functionalizing porous zirconium terephthalate UiO-66(Zr) for natural gas upgrading: a computational exploration, *Chem. Commun.*, 2011, **47**, 9603-9605.